

Further experiments on the quantum oscillations in the transport properties of aluminum

R. Fletcher

Physics Department, Queen's University, Kingston, Ontario K7L 3N6, Canada

(Received 4 August 1983)

Previous work concerning the quantum oscillations in the transverse coefficients of Al (electrical, thermal, and thermoelectric) has been extended to the off-diagonal components, i.e., the Hall and Righi-Leduc resistivities ρ_{yx} and γ_{yx} and the Nernst-Ettingshausen coefficient P_{yx} . The results show that the oscillations in ρ_{yx} and P_{yx} are accurately related by known expressions, and, providing averages for both field directions are used (i.e., $\pm B$ data), then the oscillations in γ_{yx} are also related to those in ρ_{yx} and P_{yx} . However, the individual $+B$ and $-B$ data for γ_{yx} exhibit unexplained anomalies. It has also been possible to extract the open-orbit contribution to ρ_{yx} and it is found that it is responsible for most of the oscillation amplitude when the magnetic field is close to, but not parallel to, a crystallographic cubic-symmetry axis, e.g., [100].

I. INTRODUCTION

In a previous paper¹ (subsequently referred to as I) it was shown that the quantum oscillations in the electrical resistivity ρ , the thermal resistivity $\underline{\gamma}$, and the thermoelectric tensor \underline{P} of any metal should be intimately related. These tensors are defined according to the equations

$$\vec{E} = \rho \vec{J} + \underline{P} \vec{U}, \quad \vec{\nabla} T = \underline{\Pi} \vec{J} - \underline{\gamma} \vec{U},$$

where \vec{E} and $\vec{\nabla} T$ are the electric field and temperature gradient, respectively, and \vec{J} and \vec{U} are the electrical and thermal currents; $\underline{\Pi}$ is a tensor of no particular interest in this work because it contains no new information. The theory presented in I showed that for elastic scattering, the oscillatory parts of ρ , $\underline{\gamma}$, and \underline{P} , denoted by $\tilde{\rho}$, $\tilde{\underline{\gamma}}$, and $\tilde{\underline{P}}$, are related by

$$\tilde{\underline{\gamma}} L_0 T = \alpha \tilde{\rho}, \quad (1)$$

$$\tilde{\underline{P}} L_0 T = -\beta \tilde{\rho}, \quad (2)$$

where L_0 is the Sommerfeld value of the Lorenz number, T is the temperature, and α and β are defined by the equations

$$\alpha = -3 \frac{D''(X)}{D(X)}, \quad \beta = \pm i(\pi k/e) \frac{D'(X)}{D(X)}.$$

The quantity $\pm i$, is a phase factor discussed in I, the function $D(X)$ is $X/\sinh X$, with the prime denoting differentiation with respect to X , and $X = 2\pi^2 k T m^* / \hbar e B$, B being the flux density, m^* the cyclotron mass of the orbit of interest, and the other constants having their usual significance. These predictions were tested on the transverse coefficients $\tilde{\rho}_{xx}$, $\tilde{\underline{\gamma}}_{xx}$, and \tilde{P}_{xx} of Al and found to hold to within the experimental accuracy of a few percent. In other words, if any of these three quantities is measured as a function of field, the others can be predicted very accurately over the same field range. In the derivation of Eqs. (1) and (2) there is no attempt to explore the microscopic origin of the oscillations. The theory should be equally appropriate to all the other tensor components and it is

the primary purpose of the present work to extend the experimental investigation to the oscillatory parts of the off-diagonal components, i.e., the Hall resistivity $\tilde{\rho}_{yx}$, the Right-Leduc resistivity $\tilde{\underline{\gamma}}_{yx}$, and the Nernst-Ettingshausen coefficient \tilde{P}_{yx} . Oscillations in P_{yx} have been observed previously² in Al, but there is no record that they have been seen in ρ_{yx} and γ_{yx} ; this is not too surprising since the amplitudes of $\tilde{\rho}_{yx}$ and $\tilde{\underline{\gamma}}_{yx}$ are very small, being no more than 2% of the monotonic parts in this work. On the other hand, \tilde{P}_{yx} is very large and overwhelms the monotonic part. The large amplitude of \tilde{P}_{yx} is a signature of magnetic breakdown since for normal metals the Nernst-Ettingshausen coefficient is essentially monotonic.³

In the course of this work it became obvious that the off-diagonal coefficients were showing some interesting behavior unrelated to the primary objectives outlined above. In particular it was found that each was composed of both a "normal" antisymmetric part (which reverses as the sign of B is changed) and a symmetric part (which does not reverse with B). The latter part is a direct consequence of the presence of open orbits in Al, and although we have not made an extensive study of this aspect, some data is presented to indicate its potential interest and usefulness.

II. EXPERIMENTS AND RESULTS

The sample was cut from the same single crystal as used in I and was essentially identical in size and shape except for the addition of a pair of transverse limbs to enable the off-diagonal coefficients to be measured. The residual resistance ratio was again about 850 and was intentionally chosen to be low for reasons connected with the effects of the lattice conductivity as discussed in I; it was later realized that this constraint is not important for the coefficients studied here and a purer sample would probably have been equally appropriate.

Most of the data-collection techniques were unchanged but some new features are worth recording. As will be seen later, the amplitudes of the oscillatory components in

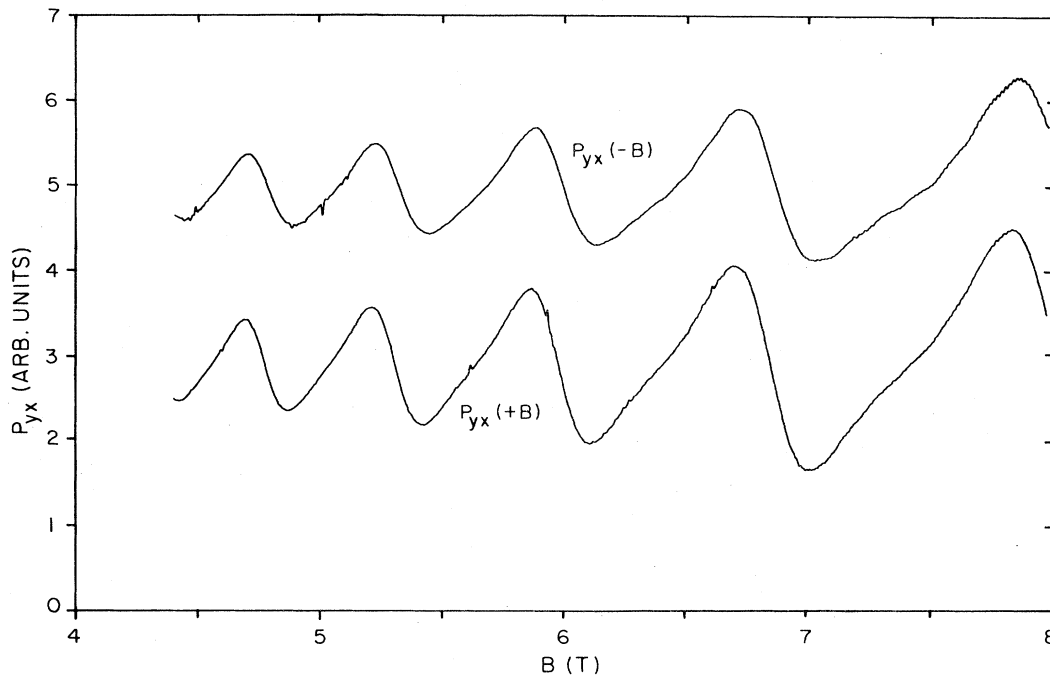


FIG. 1. Nernst-Ettingshausen coefficient P_{yx} as a function of magnetic field B at approximately 3.63 K. The graphs are actually the voltage output of the transverse probes for a fixed heat current of about 16 mW through the sample. Each ordinate unit represents about 82 nV, but the scale may be converted to mA^{-1} by multiplying by 6.96×10^{-9} (though the zeros are arbitrary for each graph). It will be noticed that the waveform is basically symmetric in B .

the off-diagonal coefficients are practically identical to those in the diagonal components investigated in I. However, sample geometrical factors result in the actual signals being about a factor of 5 smaller. To increase the signal-to-noise ratio, particularly for ρ_{yx} , a signal-averaging device was incorporated into the system. Output voltages were converted to a frequency by a voltage-to-frequency converter with excellent linearity and stability (Model No. VFC32, Burr-Brown Co., Tucson, Arizona), and the output counted for a suitable time interval. In practice, averaging times of 10 sec were usually used. Naturally very slow field sweeps are required so that the averaging time does not appreciably reduce the oscillatory amplitude; the very low frequency of the oscillation in Al is a distinct advantage in this regard.

In the case of ρ_{yx} and γ_{yx} it was often convenient to eliminate the monotonic contributions and isolate the oscillatory part for ease of analog recording and visual inspection. Because the field B is ramped linearly and both ρ_{yx} and γ_{yx} are closely proportional to B , the magnitudes of the monotonic parts are essentially linear in time. These were removed by simply subtracting a voltage of about the right magnitude produced by a linear ramp circuit. This ramp was generated by a high-resolution digital-to-analog converter driven from a stable oscillator and counter.

As previously, the orientation of \vec{B} was always close to [100] but the precise orientation was unknown except for an early run where the [100] axis was located, as will be mentioned again later. The maximum amplitude of the

oscillations occurs with \vec{B} about 1° from [100] and this maximum position was located by trial and error during the first few runs so as to secure the best signal-to-noise ratio.

Figure 1 is an example of the data taken on P_{yx} . As with P_{xx} any monotonic part is small and swamped by the oscillations. Figures 2 and 3 show examples of ρ_{yx} both with and without removal of the monotonic part, and Fig. 4 is typical of the oscillatory part of γ_{yx} , the monotonic part having been removed. In all cases the oscillatory parts are very similar in both form and magnitude to those observed in P_{xx} , ρ_{xx} and γ_{xx} and presented in I.

It is immediately evident from Figs. 1–4 that none of the oscillatory parts of the coefficients change sign when \vec{B} is reversed. This means that each coefficient must contain a symmetric part (even in B) and an antisymmetric part (odd in B) with the former dominating. A misalignment of the transverse sample limbs would introduce a spurious symmetric part to all the coefficients, e.g., ρ_{yx} would contain a contribution from ρ_{xx} . However, to obtain the observed magnitudes, this offset would need to be about 2.6 mm which is at least a factor of 20 larger than could be considered reasonable. A simple auxiliary check is to measure the transverse voltage at zero field. This was done and it was found that the apparent field E_y due to the misalignment was about 0.9% of E_x , which implies an offset of about 0.02 mm. These results indicate that the spurious offsets are negligible in this work and the symmetric parts of the coefficients are real features of the data.

III. ANALYSIS AND DISCUSSION

A. General features

All of the data are readily separated into the symmetric and antisymmetric parts, but the most useful coefficient is ρ_{yx} , since both the monotonic and oscillatory parts are available with reasonable precision. Presumably γ_{yx} contains the same information but it is difficult to obtain the same linearity and resolution in this coefficient as is achievable with ρ_{yx} . By taking data for all combinations of $\pm B_z$ and $\pm I_x$, I_x being the sample current, the symmetric and antisymmetric parts ρ_{yx}^s and ρ_{yx}^a are easily separated using the relations

$$\rho_{yx}^s = \frac{1}{2} [\rho_{yx}(+B) + \rho_{yx}(-B)]$$

and

$$\rho_{yx}^a = \frac{1}{2} [\rho_{yx}(+B) - \rho_{yx}(-B)],$$

where $\rho_{yx}(+B)$ and $\rho_{yx}(-B)$ are obtained by simple subtraction of the data sets for $\pm I_x$ for a given direction of B (which eliminates any induced emf contributions). Figure 5 shows ρ_{yx}^s obtained in this manner and it will be noticed that it is comprised of both monotonic $\bar{\rho}_{yx}^s$ and oscillatory parts $\tilde{\rho}_{yx}^s$ with similar magnitudes. The antisymmetric part ρ_{yx}^a shows very little oscillatory behavior and was analyzed by making a least-mean-squares fit to $\rho_{yx}^a = R_H B$ where R_H represents an average Hall coefficient. The measured value of R_H over the range 4.4–8 T is $1.022 \times 10^{-10} \text{ m}^3 \text{ C}^{-1}$, with an absolute uncertainty of about 1.5% mainly arising from the sample thickness measurement. For convenience, $\bar{\rho}_{yx}^a$ is defined as $\rho_{yx}^a - R_H B$ and is also shown in Fig. 5. However, it will be observed that $\bar{\rho}_{yx}^a$ does not appear to be purely oscillatory, but contains a monotonic contribution increasing with B and of the same sign as the monotonic part $R_H B$ already

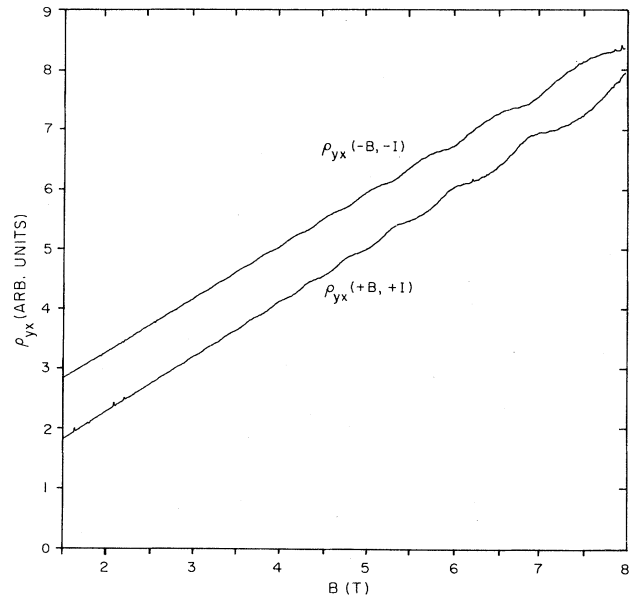


FIG. 2. Hall resistivity ρ_{yx} as a function of B at 4.2 K. The traces are actually recordings of the transverse voltage output of the sample for a fixed current of 1 A with each ordinate unit being about 82 nV. The ordinate scale may be converted to $\Omega \text{ m}$ by multiplication by 1.12×10^{-10} . The zeros are displaced by induced emf's and also intentionally to separate the curves. Although the monotonic part of ρ_{yx} is basically antisymmetric in B , the slight convergence of the lines at high B indicates a symmetric contribution. The oscillatory part is primarily symmetric in B .

subtracted. The ratio of the amplitudes of $\tilde{\rho}_{yx}^s$ and $\tilde{\rho}_{yx}^a$ is about 5. As far as our limited data indicates, $\tilde{\rho}_{yx}^a$ is not too sensitive to angle (over the available range of $\lesssim 1^\circ$) but ρ_{yx}^s depends strongly on angle, and, of course, should

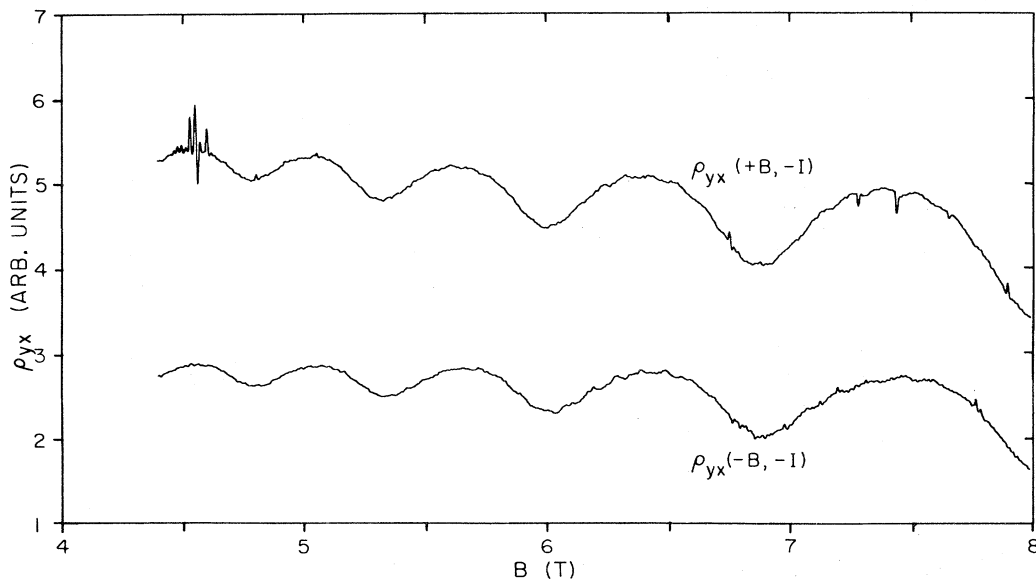


FIG. 3. Data for ρ_{yx} at 4.2 K similar to that of Fig. 2 but with the monotonic parts removed as described in the text. The ordinate scale may be converted to $\Omega \text{ m}$ by multiplication by 2.24×10^{-11} .

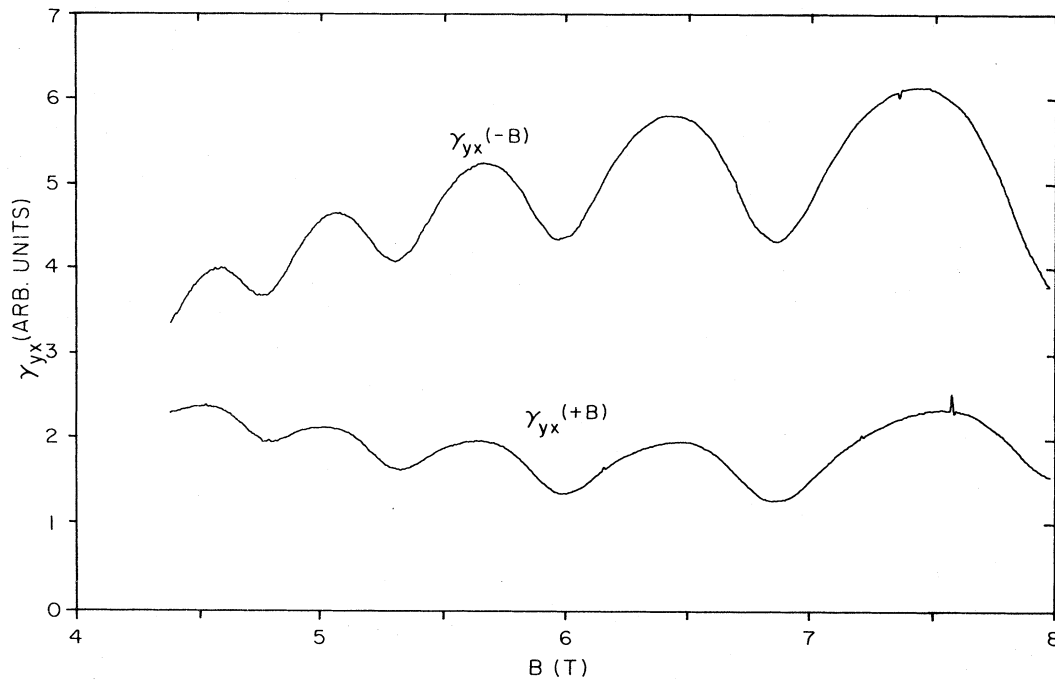


FIG. 4. Oscillatory part of the Right-Leduc coefficient γ_{yx} at 2.13 K. The recording is actually the out-of-balance output of the carbon-resistor bridge containing both the transverse thermometers with a fixed heat current of about 11.4 mW through the sample; each ordinate unit represents about 1.85 mK and may be converted to units of mK W^{-1} by multiplication by 2.21×10^{-4} . The curvature of the background is basically due to nonlinearity of the carbon thermometers as a function of T . Again, the oscillations are primarily symmetric in B , but notice that the relative amplitudes for $\pm B$ are contrary to those in P_{yx} and ρ_{yx} in Figs. 1 and 3.

disappear for $\vec{B} \parallel [100]$ because of symmetry requirements. Such behavior was observed in one of the early runs and was used to identify the $[100]$ axis. (The identification was actually made using \vec{P}_{yx} which exhibits a much better signal-to-noise ratio but the principal is the same.) A final experimental observation is that $\vec{\rho}_{yx}^s$ and $\vec{\rho}_{yx}^a$ are not quite in phase as Fig. 5 clearly shows. Detailed curve fitting indicates a phase shift of about 0.5 rad which is consistently observable in all the coefficients, e.g., when fitting \vec{P}_{yx} for $\pm B$ there is always a slight phase shift presumably attributable to the phase difference between the symmetric and antisymmetric parts.

The experimental results are consistent with the assumption that magnetic breakdown is responsible for the oscillations in ρ_{yx} . In the absence of breakdown the high-field Hall conductivity σ_{xy} is given by

$$\sigma_{xy} = (n_h - n_e)e/B = -\sigma_{yx},$$

where n_h and n_e are the densities of holes and electrons, respectively. Any oscillations in σ_{xy} should be unobservable since $n_h - n_e$ is a constant for all practical purposes.⁴ Thus for $B \rightarrow \infty$, $\rho_{xy} = 1/\sigma_{xy}$ should also be monotonic. For $\vec{B} \parallel [100]$, breakdown leads to a narrow layer of hole-like orbits being converted to electronlike orbits which produces an increase in $1/\sigma_{xy}$ and the Hall coefficient R_H .⁵ It is further found that σ_{xy} (and also ρ_{yx}) oscillates because the breakdown probability is modulated by phase coherence of the electrons on a small part of the third-zone Fermi surface⁵ which links the orbits on the second-

zone sheets by magnetic breakdown. The percentage modulation is low because the number of electrons produced by this mechanism is small over the available field range.

As \vec{B} is tipped away from $[100]$ open orbits become possible which will produce a symmetric contribution to ρ_{yx} , i.e., ρ_{yx}^s . Kesternich and Papastaikoudis⁶ have enumerated the breakdown possibilities in Al for \vec{B} tipped in a (001) or (011) plane (to give open orbits along $[001]$ and $[011]$, respectively), but presumably other angles are not excluded. Although the orbits are open, they are rather complex in nature and approach the given directions only under conditions of high fields and/or long mean free path. With the assumption of a simple linear open orbit inclined at an angle θ in reciprocal space to the applied electric field \vec{E} , the conductivity has the form,⁴ for $B \rightarrow \infty$,

$$\underline{\sigma} = \begin{bmatrix} a \sin^2 \theta & a \sin \theta \cos \theta & 0 \\ a \sin \theta \cos \theta & a \cos^2 \theta & 0 \\ 0 & 0 & b \end{bmatrix} + \begin{bmatrix} A/B^2 & C/B & 0 \\ -C/B & A/B^2 & 0 \\ 0 & 0 & A_3 \end{bmatrix}, \quad (3)$$

where the first matrix corresponds to the effects of the open orbit and the second matrix corresponds to all the closed orbits (and assumes for simplicity the symmetry appropriate to a cube axis) with $C = (n_h - n_e)e$. As before, C will show oscillations because some of the orbits produced by breakdown will still be closed, but a will also os-

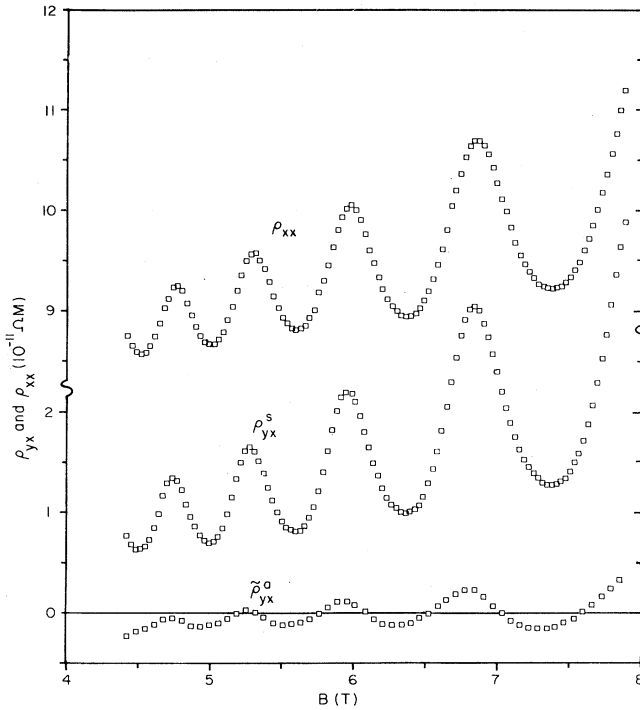


FIG. 5. The bottom curve is the oscillatory component of the antisymmetric part of the Hall resistivity ($\tilde{\rho}_{yx}^a$) defined, as explained in the text, as $\tilde{\rho}_{yx}^a = \rho_{yx}^a - R_H B$. The middle curve is the symmetric part of the Hall resistivity ρ_{yx}^s ; both oscillatory and monotonic parts are shown. The upper curve is the transverse resistivity ρ_{xx} shown for comparison with ρ_{yx}^s (notice the break in scale). All data are taken at 4.2 K; results for ρ_{yx}^a and $\tilde{\rho}_{yx}^a$ are taken from one run, and those for ρ_{xx} from another run, but the sample orientations should be identical to within 0.1° .

cillate for the same reason as C , i.e., the open orbits are linked by the same small third-zone surface on which the electrons exhibit phase coherence. Inversion of Eq. (3) gives the resistivity ρ_{ij} ,

$$\rho = \frac{aB^2}{Aa + C^2} \begin{pmatrix} \cos^2\theta & -\sin\theta \cos\theta \\ -\sin\theta \cos\theta & \sin^2\theta \end{pmatrix} + \frac{1}{Aa + C^2} \begin{pmatrix} A & -CB \\ CB & A \end{pmatrix}, \quad (4)$$

where we have reduced the matrices to 2×2 since the other components are not relevant to this discussion. Although we do not know the exact angle θ appropriate to the present work, the oscillation amplitude in ρ_{yx} was maximized by a trial-and-error adjustment of the sample axis relative to \vec{B} . This suggests that the angle actually obtained was always near $\theta = \pi/4$ which maximizes $\sin\theta \cos\theta$. If this is correct, then both ρ_{xx} and ρ_{yx} contain a term $aB^2/2(Aa + C^2)$, and in the latter case this is just ρ_{yx}^s . In the case of ρ_{xx} this term cannot be separated from any oscillatory part of $A/(Aa + C^2)$, but even so it is of interest to compare ρ_{xx} and ρ_{yx}^s —this is done in Fig. 5.

The correspondence is quite striking and supports the view that the major oscillatory part of ρ_{xx} , along with most of the monotonically increasing part of ρ_{xx} , is primarily due to the open-orbit conduction.

The behavior of the antisymmetric component ρ_{yx}^a is also of interest. This corresponds to the component $CB/(Aa + C^2)$. It will be recalled that the mean slope, R_H of ρ_{yx}^a vs B has the value $(1.022 \pm 0.015) \times 10^{-10} \text{ m}^3 \text{ C}^{-1}$. Assuming one hole per Al atom the Hall constant of Al should be $1.023 \times 10^{-10} \text{ m}^3 \text{ C}$. These values are identical, perhaps somewhat fortuitously, and imply, as expected, that breakdown effects are small in ρ_{yx}^a . Magnetic breakdown will influence ρ_{yx}^a through both the factor Aa in the denominator and also through the factor C , since breakdown will convert some holelike orbits to electronlike orbits; these effects work in opposition since the latter increases the value of R_H but the former decreases it (A and a are both positive quantities). Experiment shows that R_H increases slightly, the effect being less than 1%; presumably C dominates. This experiment would be much more usefully carried out for $\vec{B} \parallel [100]$ where open-orbit effects are absent, i.e., $a=0$.

The phase difference between $\tilde{\rho}_{yx}^a$ and $\tilde{\rho}_{yx}^s$ is most easily interpreted as being a slight frequency (i.e., area) difference of about 1% between the orbits responsible for the oscillations, as might be expected if they are not exactly in the same plane.

To summarize the situation for \vec{B} tipped slightly from $[100]$, it is reasonable to assume that most of the oscillatory contribution to ρ_{xx} and ρ_{yx} is caused by the presence of open orbits. In the latter case this corresponds to ρ_{yx}^s . The antisymmetric part of ρ_{yx} and a small fraction of ρ_{xx} are due to closed-orbit contributions which are rather insensitive to angle, at least for $\theta \lesssim 1^\circ$.

There seems to be little more that can be usefully accomplished with the data in hand, though the work suggests an interesting avenue for future investigation. In passing we note that the Right-Leduc coefficient γ_{yx} shows the same overall behavior as ρ_{yx} , though the accuracy of measurement is lower. As a matter of record, the monotonic antisymmetric parts obey the relationship $\tilde{\rho}_{yx}^a = \tilde{\gamma}_{yx}^a L_0 T$ with a discrepancy in the worst case of 1.3%, though $\tilde{\gamma}_{yx}^a$ is consistently the smaller. Presumably the differences simply reflect experimental errors since the only obvious physical reason for any discrepancy is the effect of the lattice conductivity⁷ on γ_{yx} , and an estimate shows any deviations from this source to be unobservable in this sample.

B. Amplitudes of the oscillatory components

This part of the analysis parallels that made for \tilde{P}_{xx} , $\tilde{\rho}_{xx}$, and $\tilde{\gamma}_{xx}$ in I. A total of seven experimental runs were made on \tilde{P}_{yx} , $\tilde{\rho}_{yx}$, and $\tilde{\gamma}_{yx}$ over the ranges $4 < B < 8 \text{ T}$ and $1.8 < T < 4.2 \text{ K}$. In each run the small range of available angles was scanned to find the maximum amplitude in \tilde{P}_{yx} . In the last four runs this maximum was an absolute maximum, but in the first three no such orientation could be found and the largest available amplitude was chosen. There was no attempt to separate the symmetric and an-

TABLE I. Observed values of the reduced coefficients $(C_a/A_1)(\pi k/3e)$ and $-(E_1/A_1)(L_0/3)$, both of which should be unity according to theory. Data are presented for $\pm B$ and in the case of $-(E_1/A_1)(L_0/3)$, the average values for $\pm B$ are shown in parentheses beneath the individual results. ρ_{yx} was usually measured at 4.2 K, and γ_{yx} and P_{yx} were measured at the same approximate temperatures as listed.

Run	$(C_1/A_1)(\pi k/3e)$		$-(E_1/A_1)(L_0/3)$		Approximate T (K)
	+B	-B	+B	-B	
1	0.950				3.98
2	0.977				3.91
3	1.028				3.83
4	0.987	0.993	0.757	1.150	3.63
			(0.953)		
5 and 6	0.990	0.971	0.837	1.087	3.90
			(0.962)		
		0.977	0.784	1.067	3.34
			(0.925)		
	1.003	0.980	0.690	1.227	2.75
			(0.959)		
	1.021				2.25
7	1.011	0.986	0.608	1.340	2.13
			0.465	1.423	1.80
			(0.944)		
Mean values	0.990 \pm 0.021		0.953 \pm 0.17 ^a		

^aError is that for the mean values for $\pm B$, not the individual +B and -B values.

tisymmetric parts in the following analysis. As in I, the data on $\tilde{P}_{yx}T$ were fitted first using the expression

$$\tilde{P}_{yx}T = \sum_{n=1}^3 C_n D'(nX) \exp(-B_n/B) \sin\{n[(2\pi f/B) + \phi]\},$$

with the eight unknowns C_n , B_n , f and ϕ . A simple linear term was adequate to account for the monotonic background. The data fits were always excellent and similar in quality to those shown for $\tilde{P}_{xx}T$ in I. Having obtained these unknowns, $\tilde{\rho}_{yx}$ and $\tilde{\gamma}_{yx}$ were fitted to

$$\tilde{\rho}_{yx} = \sum_{n=1}^3 A_1 (C_n/C_1) D(nX) \exp(-B_n/B) \times \cos\{n[(2\pi f/B) + \phi]\},$$

$$\tilde{\gamma}_{yx}T = \sum_{n=1}^3 E_1 (C_n/C_1) D''(nX) \exp(-B_n/B) \times \cos\{n[(2\pi f/B) + \phi]\},$$

with single unknowns A_1 and E_1 . The backgrounds were represented by low-order polynomials. These procedures were carried out independently for the $\pm B$ data. An examination of Eqs. (1) and (2) shows that it is convenient to present the final results as ratios of the coefficients in the form $(C_1/A_1)(\pi k/3e)$ and $-(E_1/A_1)(L_0/3)$, both of which should be unity if the theory is adequate.

The results of the analysis are shown in Table I. In the case of \tilde{P}_{yx} and $\tilde{\rho}_{yx}$ the agreement with the expected value of unity is excellent, regardless of the sign of B , i.e., the theory seems to be appropriate to both the symmetric and

antisymmetric parts. Calibration errors and a 1% uncertainty in m^* (see I) add to the total estimated uncertainty to give a final result of

$$(C_1/A_1)(\pi k/3e) = 0.990 \pm 0.035.$$

On the other hand, although the average result for the ratio $-(E_1/A_1)(L_0/3)$ at 0.95 ± 0.04 (the error including the effect of a 1% uncertainty in m^* and another 1% for systematic thermometer calibrations) is consistent with the expected value of unity, the ratio for -B values is always too large and that for +B values too small. This is quite evident even for the raw data of Fig. 4 as compared to that of Fig. 3. The discrepancies diverge as T is reduced but the average of $\pm B$ data at any T is remarkably constant. In spite of the amplitude problems, the fitted curves to $\tilde{\gamma}_{yx}(+B)$ and $\tilde{\gamma}_{yx}(-B)$ are good and not significantly inferior to those for $\tilde{\gamma}_{xx}$ in I. The obvious interpretation is that it is an experimental artifact, but no mechanism has been found which could lead to this behavior. It will be recalled that we find $\tilde{\gamma}_{yx}^a L_0 T = \tilde{\rho}_{yx}^a$ to within 1.3%, and although one must average $\pm B$ data to obtain this result, the separate $\pm B$ data obey this relationship to practically the same accuracy. Thus there are no calibration problems of the scale required to explain the behavior of $\tilde{\gamma}_{yx}$. Two other possibilities which were also rejected will also be mentioned. The first is that there is a contribution from $\tilde{\gamma}_{xx}$ because the transverse probes are not directly opposite for the thermal coefficient. The imbalance required is in excess of 1 mm, and worse, would have to be temperature dependent; both of these requirements are unreasonable. Finally there is a thermoelectric correction to $\tilde{\gamma}_{yx}$ which is dropped in deriving Eq. (1). Using the definitions in I one finds

$$\vec{U} = (\pi'' \sigma^{-1} \epsilon'' - \lambda'') \vec{\nabla} T,$$

which is approximated as $\vec{U} = -\lambda'' \vec{\nabla} T$. However, the phase and harmonic content of the oscillatory parts of λ'' and $\pi'' \sigma^{-1} \lambda''$ should be quite different. The oscillations in the latter will mainly arise in the thermoelectric terms π'' and ϵ'' and should be shifted by $\pi/2$ compared to those in λ'' . Furthermore, because of the product terms in $\pi'' \sigma^{-1} \epsilon''$, we would not expect to see a fundamental of significant magnitude in the harmonic series, the first term being the second harmonic $2f$. In other words, although the magnitude of this correction term is very difficult to estimate, it does not have the characteristics required to plausibly explain the anomalies.

IV. CONCLUSIONS

Equations (1) and (2) should be appropriate to all components of the tensors $\tilde{\rho}$, $\tilde{\gamma}$, and \tilde{P} . In I it was shown that these relationships are accurately obeyed for the transverse coefficients $\tilde{\rho}_{xx}$, $\tilde{\gamma}_{xx}$, and \tilde{P}_{xx} . The present work indicates that the equations are equally valid for the off-diagonal components $\tilde{\rho}_{yx}$ and \tilde{P}_{yx} , and with some reservations for

$\tilde{\gamma}_{yx}$. We have no acceptable explanation for the behavior of $\tilde{\gamma}_{yx}$ with $+B$ and $-B$, but there is no doubt that the mean data for $\pm B$ is in good agreement with Eq. (1). The only other major components which remain to be examined are the longitudinal coefficients $\tilde{\rho}_{zz}$, $\tilde{\gamma}_{zz}$, and \tilde{P}_{zz} ; these will require very sensitive techniques because the absolute amplitudes of the oscillations are expected to be very small for $\tilde{\rho}_{zz}$ and $\tilde{\gamma}_{zz}$.

The present work has also demonstrated the usefulness of ρ_{yx} in investigating open-orbit effects in the presence of breakdown. It is clear that for small deviations of \vec{B} from a cubic axis (say [100]), the major oscillatory effects in all of ρ_{yx} , P_{yx} , and γ_{yx} for Al are caused by the open-orbit contribution. A careful examination of ρ_{yx} to determine the symmetric component ρ_{yx}^s should give unambiguous information concerning the range of angles for which open orbits are possible in Al and other metals.

ACKNOWLEDGMENT

The work was supported by the Natural Sciences and Engineering Research Council of Canada.

¹R. Fletcher, Phys. Rev. B **28**, 1721 (1983).

²C. Papastaikoudis and W. Kesternich, Phys. Rev. B **17**, 2518 (1978).

³R. Fletcher, Can. J. Phys. **60**, 122 (1982).

⁴A. B. Pippard, Rep. Prog. Phys. **23**, 176 (1960).

⁵R. J. Balcombe and R. A. Parker, Philos. Mag. **21**, 533 (1970).

⁶W. Kesternich and C. Papastaikoudis, J. Phys. F **7**, 837 (1977).

⁷R. Fletcher, J. Phys. F **4**, 1155 (1974).